

Tuning Mixing within a Droplet for Digital Microfluidics

R. Chabreyrie^a D. Vainchtein^{b,c} C. Chandre^d P. Singh^e

N. Aubry^a

^a*Mechanical Engineering Department, Carnegie Mellon University, Pittsburgh, PA
15213, USA*

^b*School of Physics, Georgia Institute of Technology, GA 30332, USA*

^c*Space Research Institute, Moscow, GSP-7, 117997, Russia*

^d*Centre de Physique Théorique, CNRS – Aix-Marseille Universités, Luminy-case
907, F-13288 Marseille cedex 09, France¹*

^e*Mechanical Engineering Department, New Jersey Institute of Technology,
Newark, NJ 07102, USA*

Abstract

The design of strategies to generate efficient mixing is crucial for a variety of applications, particularly digital microfluidic devices that use small “discrete” fluid volumes (droplets) as fluid carriers and microreactors. In recent work, we have presented an approach for the generation and control of mixing inside a translating spherical droplet. This was accomplished by considering Stokes’ flow within a droplet proceeding downstream to which we have superimposed time dependent (sinusoidal) rotation. The mixing obtained is the result of the stretching and folding of material lines which increase exponentially the surface contact between reagents. The mixing strategy relies on the generation of resonances between the steady and

the unsteady part of the flow, which is achieved by tuning the parameters of the periodic rotation. Such resonances, in our system, offer the possibility of controlling both the location and the size of the mixing region within the droplet, which may be useful to manufacture inhomogeneous particles (such as Janus particles). While the period and amplitude of the periodic rotation play a major role, it is shown here by using a triangular function that the particular shape of the rotation (as a function of time) has a minor influence. This finding demonstrates the robustness of the proposed mixing strategy, a crucial point for its experimental realization.

Key words: Digital Microfluidics, Droplet, Stokes' flow, Chaotic mixing, Resonances, Control, Robustness.

PACS: 47.51.+a, 47.61.Ne, 47.52.+j

1 Introduction

Although most microfluidics have been using fluid-streams as the main means to carry fluids, devices based on individual droplets have been proposed as well. In the latter, also called “digital microfluidic” systems, “discrete” fluid volumes (droplets) rather than continuous streams are used, with the potential to utilize individual droplets as microreactors [1].

Whether fluids are encapsulated within droplets or flow along channels, reactions can occur efficiently only in presence of rapid mixing. Such mixing conditions are not easy to fulfill due to the low Reynolds number of the flow involved, which prevents turbulence from taking place. Stirring, in addition

¹ UMR 6207 of the CNRS, Aix-Marseille and Sud Toulon-Var Universities. Affiliated with the CNRS Research Federation FRUMAM (FR 2291). CEA registered research laboratory LRC DSM-06-35.

to molecular diffusion, is needed to stretch and fold fluid elements, thus significantly increasing interfacial areas. Whereas some strategies are based on complex channel geometry for flows in microchannels, active methods (via external forcing) (see, e.g. [2,3,4,5,6]) have also resulted in efficient mixing, especially at very low Reynolds numbers [7]. The combination of both geometry alteration and forcing has been explored as well [7,8,9,10,11].

Chaotic advection inside a liquid droplet subjected to a forcing has been studied extensively [12,13,14,15,16,17,18] and obtained experimentally by means of oscillatory flows [19,20]. In this paper as in [21], we concentrate on controlling both the size and the location of the mixing. Indeed, we are interested in both complete and incomplete mixing within drops. While complete mixing should be useful for efficient reactions to occur uniformly, there are applications in which non-uniform mixing, when well-controlled, could be desired. The latter include the formation of inhomogeneous drops and particles, such as Janus particles, whose properties have been shown, in certain cases, to be superior to their homogeneous counterparts. In this paper, we extend the results of [21] which were obtained by using unsteady – sinusoidal – forcing on a translating droplet. Specifically, we study the robustness of the control of the size and location of the mixing region by selecting a different time function for the rotation.

The existence of chaotic behavior in three-dimensional bounded steady flows has been shown (e.g. [12,13,23,24]). Our work is distinct from the latter contributions through the addition of unsteadiness, which is crucial to control the chaotic mixing behavior through resonance effects [25,26,18].

The physical system under consideration in this work is described in Sec. 2, and our numerical results are displayed in Sec. 3. The control of both the location (Sec. 3.1) and size (Sec. 3.2) of the chaotic mixing region is studied

qualitatively via *Liouvilian* sections.

2 Physical system

2.1 Flow equations and assumptions

Let us assume a Newtonian liquid droplet of spherical shape suspended in an incompressible Newtonian fluid. Its motion consists of a translation and a slow rigid body rotation (see [13]). As in the previous reference, we assume that the interfacial tension is sufficiently large for the drop to remain spherical through its motion and that the Reynolds number is very small compared to 1. Thus, a reasonable approximation is to consider that both the internal and external flows are Stokes flows. The boundary conditions at the droplet surface can be derived from the continuity of velocity and tangential stress conditions.

The resulting internal flow is a superimposition of a steady base flow (non-mixing flow) and an unsteady rigid-body rotation. Consider a Cartesian coordinate system translating with the center-of-mass velocity of the droplet with the orientation of the axes such that the unit vector \mathbf{e}_z points in the direction of the translation and the unit vector \mathbf{e}_x lies in the $\boldsymbol{\omega} - \mathbf{e}_z$ plane. We then obtain the following unsteady internal flow:

$$u = \dot{x} - \epsilon a_\omega(t) \omega_z y, \tag{1}$$

$$v = \dot{y} + \epsilon a_\omega(t) (\omega_z x - \omega_x z), \tag{2}$$

$$w = \dot{z} - 2\dot{x}^2 - 2\dot{y}^2 - \dot{z}^2 + \epsilon a_\omega(t) \omega_x y, \tag{3}$$

where u , v and w are the time derivatives of x , y and z , respectively. In Eqs. (1-3), all the lengths and velocities were made dimensionless by using the droplet radius and the magnitude of the translational velocity as the length

and velocity scales, respectively. The rotation is characterized by a rotation with a maximum amplitude $\epsilon \ll 1$, a fixed orientation vector

$$\boldsymbol{\omega} = (\sqrt{2}/2, 0, \sqrt{2}/2),$$

and a periodic amplitude of the rotation $a_\omega(t)$. In the present paper we study two time dependent functions for the amplitude of the rotation $a_\omega(t)$, one consisting of only one harmonic:

$$\mathcal{C}_\omega(t) = \frac{1}{2} (1 + \cos \omega t), \quad (4)$$

and the other one consisting of a triangular function with an infinite number of harmonics:

$$\mathcal{T}_\omega(t) = 1 + \sum_{n=1}^{\infty} \alpha_{2n-1} \cos((2n-1)\omega t), \quad \text{where } \alpha_n = \left(\frac{2}{n\pi}\right)^2. \quad (5)$$

Equations (1-3) are the same as in [13] except that the vorticity vector, that was constant in [13], is unsteady in our case. Note that the internal flow is a solution of the (time dependent) Stokes problem in which a time-dependent body force has been added on the right hand side of the momentum equation. In practice, this time-dependent forcing could be realized, e.g. by creating a time-dependent swirl motion in the external flow or by applying an electric field that exerts a torque on the drop (see, e.g. [27] or work on electrorotation [28]). Note that the surface of the droplet, $r^2 = x^2 + y^2 + z^2 = 1$ is invariant under flow (1-3).

2.2 Non-mixing case

The non-mixing (unperturbed) case or base flow, i.e. $\epsilon = 0$, is characterized by two invariants (i.e. time-independent quantity), the stream function ψ and

the azimuthal angle ϕ such that:

$$\psi = \frac{1}{2} (x^2 + y^2) (1 - x^2 - y^2 - z^2), \quad \phi = \arctan(y/x),$$

where $\psi \in [0, 1/8]$ and $\phi \in [0, 2\pi[$. The streamlines of the non-mixing case are joint lines of constant ψ and ϕ , denoted by $\Gamma_{\psi,\phi}$. The heteroclinic orbits $\Gamma_{\psi,\phi}$ such that $\psi = 0$ and $\phi \in [0, 2\pi[$, connect two hyperbolic fixed points located at the poles of the sphere (see Fig. 1). All other streamlines are closed curves that converge toward a circle of degenerate elliptic fixed point ($x^2 + y^2 = 1/2, z = 0$) as ψ is increased toward the value $1/8$. The frequency of motion on the streamline $\Gamma_{\psi,\phi}$ is independent of ϕ and given by

$$\frac{2\pi}{\Omega(\psi)} = \int_{-\pi/2}^{\pi/2} \frac{\sqrt{2} d\beta}{\sqrt{1 + \gamma(\psi) \sin \beta}} = \frac{2\sqrt{2}}{\sqrt{1 + \gamma}} K \left(\sqrt{\frac{2\gamma}{1 + \gamma}} \right), \quad (6)$$

with $\gamma(\psi) = \sqrt{1 - 8\psi}$ and K is the complete elliptic function of the first kind. The plot of Ω as a function of ψ , presented in Fig. 1, shows that Ω is bounded by two limits, $\Omega(0) = 0$ and $\Omega(1/8) = \sqrt{2}$. On every streamline $\Gamma_{\psi,\phi}$ we introduce a uniform phase $\chi \bmod 2\pi$ such that $\chi = 0$ on the $\mathbf{e}_x - \mathbf{e}_y$ plane and $\dot{\chi} = \Omega(\psi)$. With this uniform phase, the non-mixing flow can be described by using the variables (ψ, ϕ, χ) instead of the Cartesian coordinates (x, y, z) :

$$\dot{\psi} = 0, \quad \dot{\phi} = 0, \quad \dot{\chi} = \Omega(\psi).$$

Such a system is generally classified as *action-action-angle*, where the two invariants ψ and ϕ are the two actions and χ is the angle.

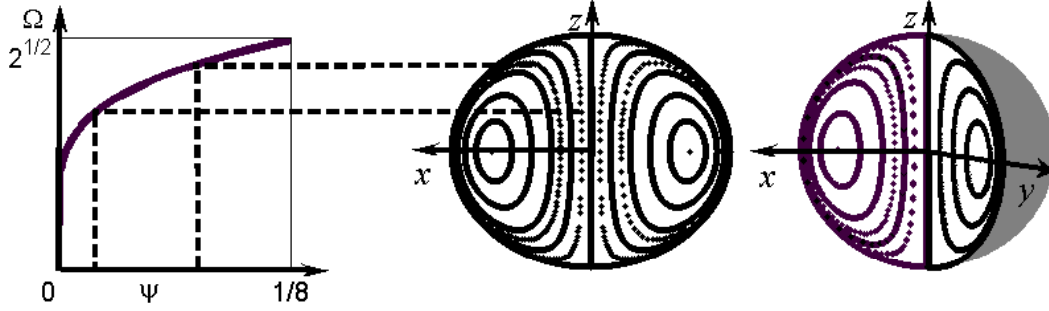


Fig. 1. Streamlines in a cross-section of the drop (without rotation) and their frequencies $\Omega(\psi)$ as given by Eq. (6).

2.3 Mixing case

In the mixing (or weakly perturbed) case $0 < \epsilon \ll 1$, the quantities ψ and ϕ are no longer constant and their time evolution satisfies

$$\dot{\psi} = -2\epsilon a_\omega(t) \omega_x \psi \sin \phi G(\psi, \chi),$$

$$\dot{\phi} = \epsilon a_\omega(t) \omega_z - \epsilon a_\omega(t) \omega_x \cos \phi G(\psi, \chi),$$

where $G(\psi, \chi) = z/(x^2 + y^2)$ is 2π periodic in χ and has zero average in χ .

The time evolution equation for χ reads

$$\dot{\chi} = \Omega(\psi) + \epsilon a_\omega(t) H(\psi, \phi, \chi),$$

where H is 2π periodic in χ . Such a system possesses two time scales, a fast one (of order one) associated with χ , typically on time scales of 1, and a slow one (of order $1/\epsilon$) associated with both ψ and ϕ . The generation of chaos arises from the resonances between the frequency of the integrable case $\Omega(\psi)$ and the forcing frequency ω .

3 Generation and control of the chaotic mixing region

In this work we follow the approach of [21] that enables the generation of a three-dimensional chaotic mixing region, for which we are able to control both the location and the size. The method consists in bringing a specific family of the unperturbed tori $\{\Gamma_{\psi_{n,m}}\}_{n,m \in \mathbb{N}^2}$ into resonance with the periodic perturbation $a_\omega(t)$ by selecting the frequency ω so that it satisfies the resonance condition:

$$n\Omega(\psi_{n,m}) - m\omega = 0, \quad \text{for } n, m \in \mathbb{N}^2.$$

The control is realized by selecting the two parameters that characterize the periodic rigid body rotation, specifically its the maximum amplitude ϵ and its frequency ω . The amplitude satisfies $0 \leq \epsilon \ll 1$, where the lower and upper limits correspond to the absence of mixing and complete mixing, respectively. In this work we are interested in the location of the mixing regions within the drop. To study our system, we compute two-dimensional projections of time-periodic three-dimensional flows via the combination of a stroboscopic map and a plane section (here, the $y = 0$ plane). In other words, the points on these so called Liouivillian sections are the intersections of the trajectories with the plane $y = 0$ at every period $2\pi/\omega$.

3.1 Control of the location

In this paper, we study the influence on mixing for two different time-dependent functions of the periodic forcing: $\mathcal{C}_\omega(t)$ that corresponds to only one harmonic and $\mathcal{T}_\omega(t)$ that is a triangular shaped forcing (see Fig. 2 and

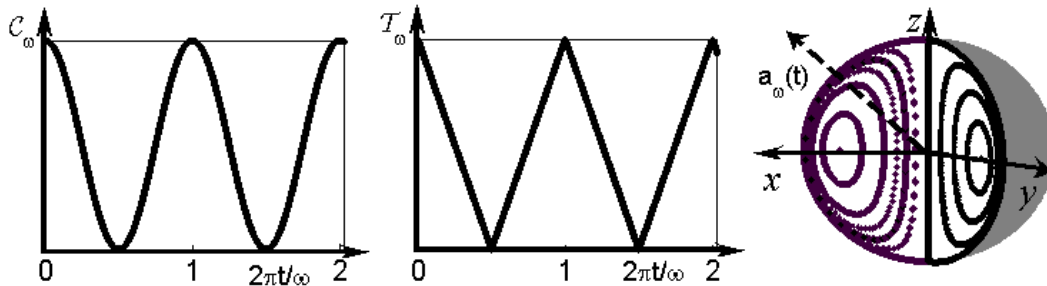


Fig. 2. Right panel: Spherical droplet represented with rigid body rotation (axis in dash line). Middle panel: Plot of the periodic forcing $\mathcal{T}_\omega(t)$ of the rigid body rotation. Left panel: Plot of the periodic forcing $\mathcal{C}_\omega(t)$ of the rigid body rotation.

Eqs. (4,5)). The two functions differ by:

$$|\mathcal{T}_\omega(t) - \mathcal{C}_\omega(t)| \leq 0.11, \quad \forall t \in \mathbb{R}.$$

Figure 3 shows the case where the periodic forcing $a_\omega(t)$ of the rigid body rotation has only one harmonic $a_\omega(t) = \mathcal{C}_\omega(t)$. Here, one can observe two major three-dimensional chaotic mixing regions, all others being of almost negligible size. The first one of these major mixing regions is around the pole-to-pole connections in the center and near the surface of the droplet. This region corresponds to the resonance of the family of unperturbed tori $\{\Gamma_{\psi_{n,1}}\}_n$ with $n > 1$ and is labeled as the central chaotic mixing region. The other one corresponds to the resonance of the unperturbed tori $\Gamma_{\psi_{1,1}}$ and is labeled as the primary chaotic mixing region. While the central mixing region is always present at this particular location inside the drop, the primary one can be displaced within the droplet. For small values of ω , the primary and central chaotic mixing regions coincide, located around the pole-to-pole connection. For larger values of ω , the primary chaotic mixing region separates from the central one, and penetrates deeper into the droplet. As ω is increased further, it moves toward the location of the circle of degenerate elliptic fixed point of

the unperturbed system ($z = 0$, $x^2 + y^2 = 1/2$) by following the location given by $\psi_{1,1}$.

Figure 4 shows the case where the periodic forcing of the rigid body rotation is $a_\omega(t) = \mathcal{T}_\omega(t)$. As in the situation where only one harmonic is present, one observes two major chaotic mixing regions. While the central region remains around the pole-to-pole connection, the primary one can be shifted across the droplet by varying the frequency ω , as it is the case for $\mathcal{C}_\omega(t)$.

Although the triangular amplitude \mathcal{T}_ω is composed by an infinite number of harmonics, only the first harmonic plays a non-negligible role. All other chaotic mixing zones created by higher harmonic appear of negligible size within the values of parameters studied. This result reinforces the robustness of the proposed method and confirms that the main parameter influencing the location of the primary mixing zone is the frequency ω , and not the specific shape of the forcing.

3.2 Control of the size

Whereas the tuning of the frequency ω of the rigid body rotation enables the placement of the primary chaotic mixing region at a particular location inside the droplet, it is its amplitude ϵ that mostly determines the size of the main mixing regions.

The sizes of the primary and central chaotic mixing regions are presented in Figs. 5,6 for the two perturbations discussed above. It is clear that in both cases the size increases with the amplitude of the rotation ϵ . Such a control of the size of the mixing allows one to vary the extent of mixing generated within the droplet from no mixing to complete mixing.

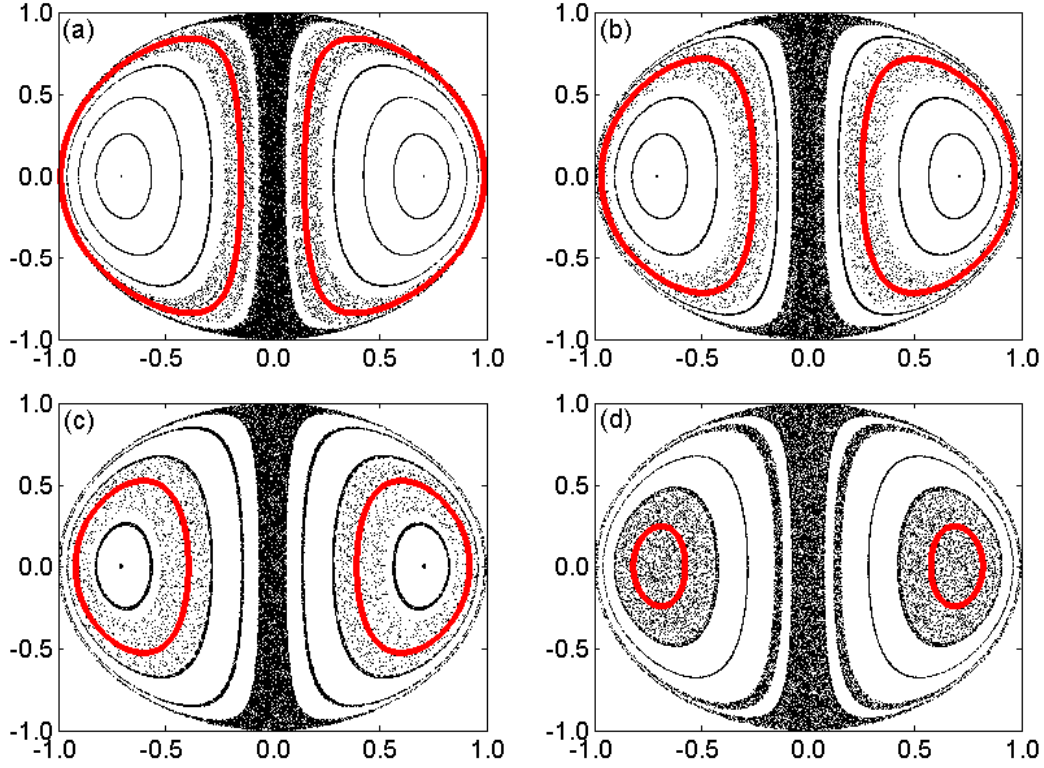


Fig. 3. (Color on line) Liouvillean sections for the time-dependence \mathcal{C}_ω with the frequencies $\omega = 0.95, 1.10, 1.25, 1.40$ (a-d) and the amplitude $\epsilon = 0.05$. The (red) dashed line inside the primary mixing region is $\Gamma_{\psi_{1,1}}$.

Once again it is important to note that for the case where the periodic amplitude of rotation is triangular only the first harmonic plays a significant role. Figure 6 shows the case of nearly no mixing ($\epsilon = 0.01$) and that of complete mixing ($\epsilon = 0.20$), the predominance of the first harmonic is not affected by the magnitude of ϵ .

4 Conclusions

In this paper, we have shown that a chaotic mixing region within a droplet is generated by adding a slow oscillatory rigid-body rotation to the translating

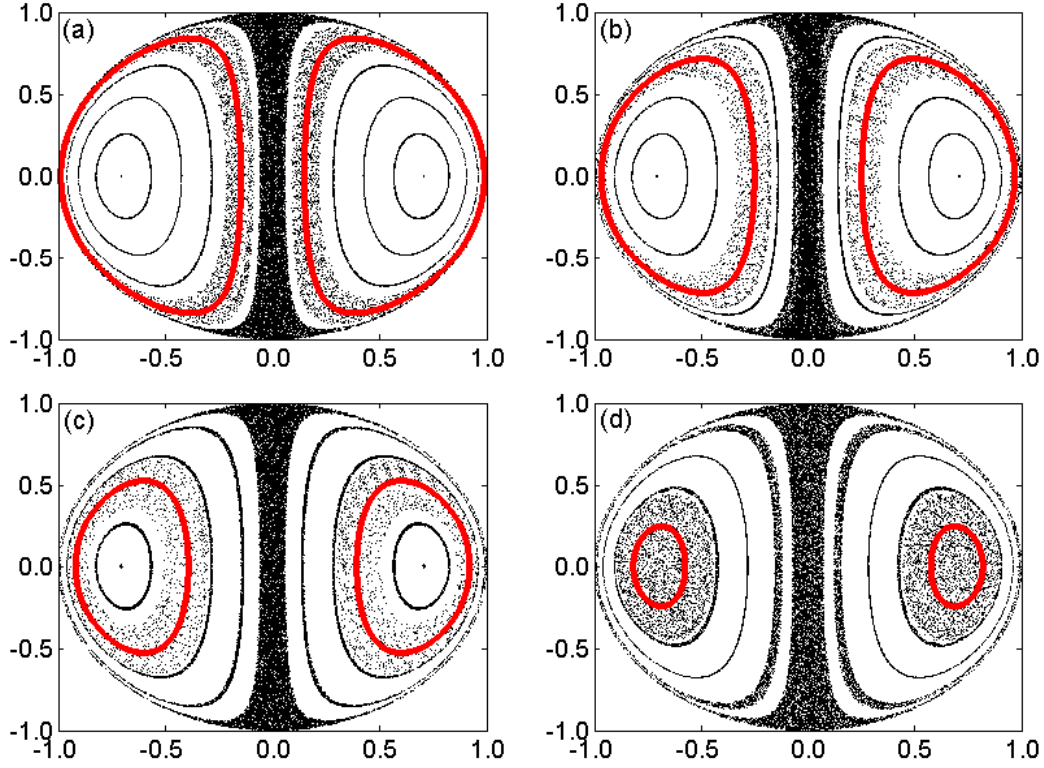


Fig. 4. (color online) Liouvillian sections for the time-dependence \mathcal{T}_ω with the frequencies $\omega = 0.95, 1.10, 1.25, 1.40$ (a-d) and the amplitude $\epsilon = 0.05$ with $a_\omega(t) = \mathcal{T}_\omega(t)$. The (red) dashed line inside the primary mixing region is the torus $\Gamma_{\psi_{1,1}}$.

drop motion. Our strategy consists in using resonances between one of the frequencies of the base flow generated by the steady translation and the forcing frequency characteristic of the oscillatory rigid body rotation. This strategy allows for a direct control of both the location and the size of the mixing by judiciously adjusting the parameters of the time-dependent rotation, i.e. its amplitude and frequency. On the one hand, controlling the mixing location could be useful to manufacture inhomogeneous droplets and particles (such as Janus particles) whose properties could be superior to homogeneous ones. On the other hand, controlling the size of the mixing zone could be important to control reaction rates. Note that in this system, the total mixing state does

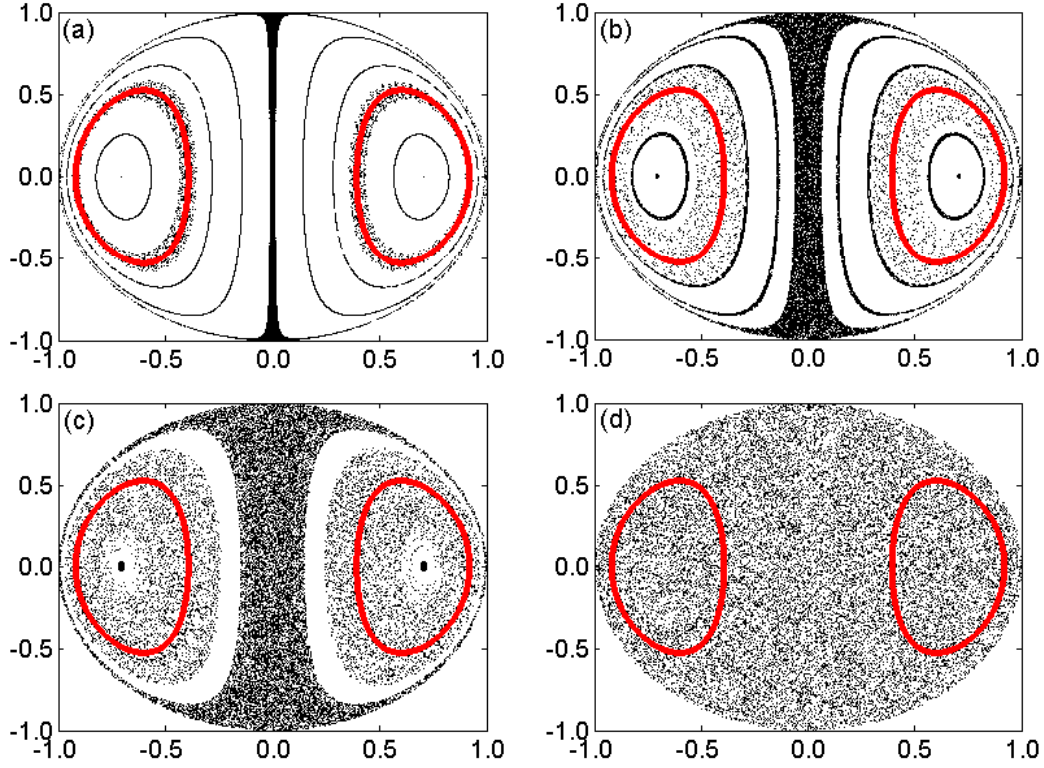


Fig. 5. (Color on line) Liouvillian sections for the time-dependence \mathcal{C}_ω with the frequencies $\omega = 1.25$ and the amplitude $\epsilon = 0.01, 0.05, 0.10, 0.20$ (a-d). The (red) dashed line inside the primary mixing region is $\Gamma_{\psi_{1,1}}$.

not have islands of non-mixing zones, as is often the case with other mixing strategies. Size and location control was obtained not only with a sinusoidal rotation (with only one harmonic) but also with a rotation consisting of a time dependent triangular function, with an infinite number of harmonics. In the latter case, the first harmonic only was shown to play a significant role.

Acknowledgements

This article is based upon work partially supported by the NSF (grants CTS-0626070 (N.A.), CTS-0626123 (P.S.) and 0400370 (D.V.)). D.V. is grateful

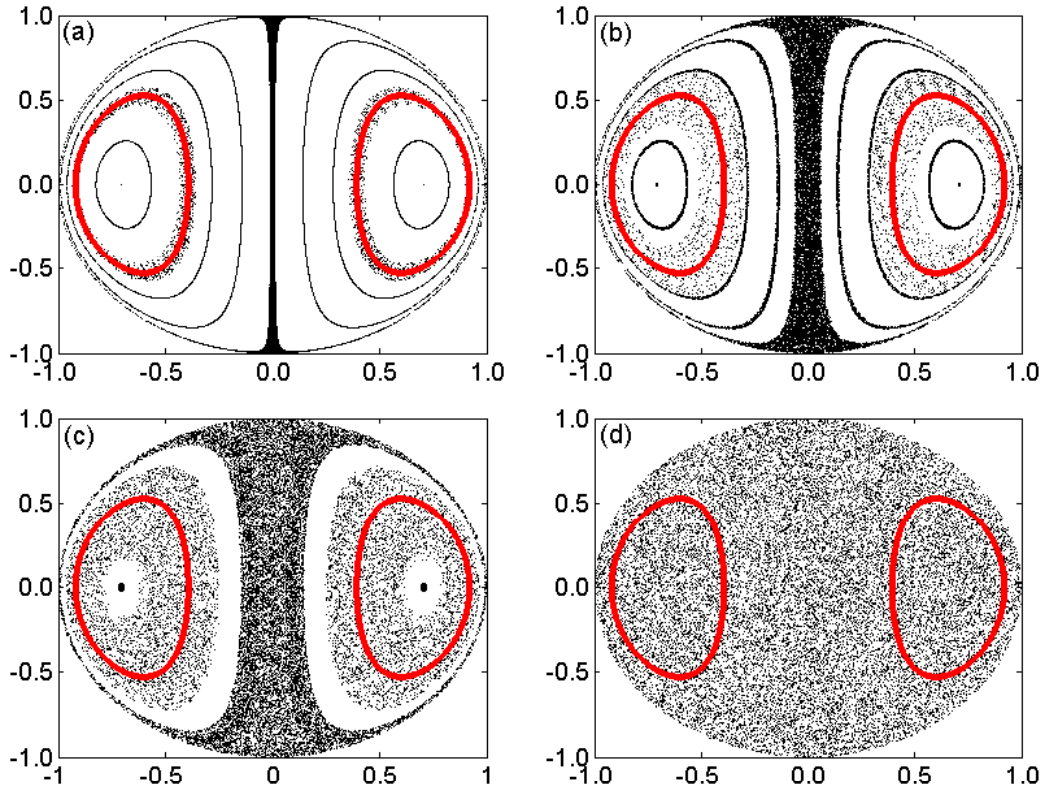


Fig. 6. (Color on line) Liouvillian sections for the time-dependence \mathcal{T}_ω with the frequencies $\omega = 1.25$ and the amplitude $\epsilon = 0.01, 0.05, 0.10, 0.20$ (a-d). The (red) dashed line inside the primary mixing region is $\Gamma_{\psi_{1,1}}$.

to the RBRF (grant 06-01-00117) and to the Donors of the ACS Petroleum Research Fund. C.C. acknowledges support from Euratom-CEA (contract EUR 344-88-1 FUA F) and CNRS (PICS program).

References

- [1] H. Song, J.D. Tice and R. F. Ismagilov, A Microfluidic System for Controlling Reaction Networks in Time, *Angew. Chem. Int. Edit.* 42, (2003) 768-772.
- [2] M.H. Oddy, J.G. Santiago, J.C. Mikkelsen, Electrokinetic Instability Micromixing, *Anal. Chem.* 73, (2001) 5822-5832.

- [3] H.H. Bau, J. Zhong and M. Yi, A minute magneto hydrodynamic (MHD) mixer, *Sens. Actuators B* 79, (2001) 207-215.
- [4] A. Ould El Moctar, N. Aubry and J. Batton, Electro-hydrodynamic microfluidic mixer, *Lab Chip* 3, (2003) 273-280.
- [5] I.K. Glasgow and N. Aubry, Enhancement of microfluidic mixing using time pulsing, *Lab Chip* 3, (2003) 114-120.
- [6] I.K. Glasgow, J. Batton and N. Aubry, Electroosmotic mixing in microchannels, *Lab Chip* 4, (2004) 558-562.
- [7] A. Goulet, I.K. Glasgow and N. Aubry, Effects of microchannel geometry on pulsed flow mixing, *Mech. Res. Commun.* 33, (2006) 739-746.
- [8] X. Niu and Y-K. Lee, Efficient spatial-temporal chaotic mixing in microchannels, *J. Micromech. Microeng.* 13, (2003) 454-462.
- [9] F. Bottausci *et al.*, Mixing in the shear superposition micromixer: three-dimensional analysis, *Phil. Trans. Royal Soc. A* 362, (2004) 1001-1018.
- [10] M.A. Stremler, F.R. Haselton and H. Aref, Designing for chaos: applications of chaotic advection at the microscale, *Phil. Trans. Royal Soc. A* 362, (2004) 1019-1036.
- [11] Y.K. Lee, C. Shih, P. Tabeling, C.M. Ho, Experimental study and nonlinear dynamic analysis of time-periodic micro chaotic mixers, *J. Fluid Mech.* 575, (2007) 425-448.
- [12] K. Bajer and H.K. Moffatt, On a class of steady confined Stokes flows with chaotic streamlines, *J. Fluid Mech.* 212, (1990) 337-363.
- [13] D. Kroujiline and H.A. Stone, Chaotic streamlines in steady bounded three-dimensional Stokes flows, *Physica D* 130, (1999) 105-132.

- [14] S.M. Lee, D.J. Im and I.S. Kang, Circulating flows inside a drop under time-periodic nonuniform electric fields, *Phys. Fluids* 12, (2000) 1899-1910.
- [15] T. Ward and G.M. Homsy, Electrohydrodynamically driven chaotic mixing in a translating drop, *Phys. Fluids* 13, (2001) 3521-3525.
- [16] R.O. Grigoriev, Chaotic mixing in thermocapillary-driven microdroplets, *Phys. Fluids* 17, (2005) 033601.1-033601.8.
- [17] X.M. Xu and G.M. Homsy, Three-dimensional chaotic mixing inside drops driven by a transient electric field, *Phys. Fluids* 19, (2007) 013102.1-013102.11.
- [18] D. Vainchtein, J. Widloski and R. Grigoriev, Resonant chaotic mixing in a cellular flow, *Phys. Rev. Lett.* 99, (2007) 094501.1-094501.4.
- [19] T. Ward and G.M. Homsy, Electrohydrodynamically driven chaotic mixing in a translating drop part II: Experiments, *Phys. Fluids* 15, (2003) 2987-2994.
- [20] R.O. Grigoriev, M.F. Schatz and V. Sharma, Optically controlled mixing in microdroplets, *Lab Chip* 6, (2006) 1369-1372.
- [21] R. Chabreyrie *et al.*, Tailored mixing inside a translating droplet, *Phys. Rev. E* 77, (2008) 036314.1-036314.4.
- [22] M. Feingold, L.P. Kadanoff and O. Piro, Passive scalars, three-dimensional volume-preserving maps, and chaos, *J. Stat. Phys.* 50, (1988) 529-565.
- [23] D. Vainchtein, A. Vasiliev and A. Neishtadt, Adiabatic chaos in a two-dimensional mapping, *Chaos* 6, (1996) 514-518.
- [24] D. Vainchtein, A. Neishtadt and I. Mezić, On passage through resonances in volume-preserving systems, *Chaos* 16, (2006) 043123.1-043123.11.
- [25] R. Lima and M. Pettini, Suppression of chaos by resonant parametric perturbations, *Phys. Rev. A* 41, (1990) 726-733.

- [26] J.H.E. Cartwright, M. Feingold and O. Piro, Chaotic advection in three-dimensional unsteady incompressible laminar flow, *J. Fluid Mech.* 316, (1996) 259-284.
- [27] N. Aubry and P. Singh, Influence of particle-particle interactions and particle rotational motions in traveling wave dielectrophoresis, *Electrophoresis* 27, (2006) 703-715.
- [28] W.M. Arnold, U. Zimmermann, Electro-rotation: development of a technique for dielectric measurements on individual cells and particles, *J. electrostat.* 21, (1988) 151-191.